

# A novel Chlorophyll Fluorescence based approach for Mowing Area Classification

Nils Rottmann<sup>1</sup>, Ralf Bruder<sup>1</sup>, Achim Schweikard<sup>1</sup>, Elmar Rueckert<sup>1</sup>

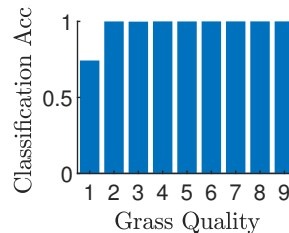
**Abstract**—Detecting cost-effectively and accurately the working area for autonomous lawn mowers is key for widespread automation of garden care. At present this is realized by means of perimeter wire, which leads to high setup and maintenance costs. Here, we propose an active low-cost sensor approach for detecting chlorophyll fluorescence response. Our novel and innovative sensing concept allows for a robust working area detection. The classification is thereby based on the averaging of multiple measurements using LED pulses and sensed fluorescence responses. By selecting only low-cost consumer components for the sensor design, we allow for high-volume production under low-cost aspects.

We evaluated our novel sensor system by analyzing theoretically the signal path. Among other we investigated sampling frequencies, sensed surface areas and environmental influences. In real world experiments, we evaluated the performance of our sensor in an exemplary garden and on collected grass samples. Our theoretical and practical evaluations show that the sensor classification result is robust under different environmental conditions, such as changes in lawn quality.

## I. INTRODUCTION

Many strategies were proposed to detect the boundaries of the working area for autonomous lawn mowers, for example vision based localization and mapping strategies [1], [2] or capacity based sensor technology for detecting humidity [3]. However, since for autonomous mowers the safety impact on leaving the mowing area is high, the sensory systems have to be reliable. Vision based system use color and texture identifiers to detect grass-containing regions using statistical methods, e.g. Bayes classifier [4] and reach accuracies of 90%, shaded grass, and 95%, illuminated grass [5]. Capacity based system have to be calibrated and are sensitive with respect to change in air conditions, such as rain or fog. In addition, there are local positioning systems which rely on active beacons using triangulation [6]. However, such local positioning systems require a-priori an exact map of the environment. The only working electronics in consumer market nowadays use bounding wire, electro-magnetic field measurement technology which safely detects wire crossing and in/outside area estimation. Such technique has been firstly introduced in lawn mowers in [7]. However, it requires the installation of a perimeter wire surrounding the lawn which results in additional time and maintenance costs. In order to overcome these problems, we introduce a cost-efficient grass detection system based on remote chlorophyll fluorescence sensing, Figure 1. A three page abstract paper, giving an

<sup>1</sup>Institute for Robotics and Cognitive Systems, University of Luebeck, Ratzeburger Allee 160, 23562 Luebeck, Germany  
{rothmann, bruder, schweikard, rueckert}@rob.uni-luebeck.de



(a) The classification accuracy for the proposed chlorophyll fluorescence sensor evaluated with different grass qualities where 1 is the lowest and 9 the best.



(b) The novel chlorophyll fluorescence based sensor. The main components are the LED for the illumination and the phototransistor for detecting the chlorophyll fluorescence response

Fig. 1: The remote chlorophyll fluorescence sensor and the classification accuracy with respect to different lawn types, Figure 11.

overview of our approach, will be presented at the IEEE Sensors conference [8].

Current remote chlorophyll fluorescence sensing systems can be grouped into ground based measurement and long distance systems [9]. The ground based measurement systems can be further partitioned into active and passive ones. The most popular group of sensors for active chlorophyll fluorescence sensing are FLiDAR (Fluorescence Light Detection and Ranging) [10], where brief periodic excitation pulses ( $< 1 \mu s$ ) with defined wavelength (e.g.  $355 nm$ ) are used for excitation. Current FLiDARs are using multiple excitation wavelength, e.g. for identifying plant species [11] or the stress level [12]. Passive remote sensing, in comparison, relies on the fluorescence induced by the natural sunlight. Since the fluorescence represents only a very small fraction of the recorded spectrum, Fraunhofer lines are used in order to measure the fluorescence signal, for example using FLD (Fraunhofer Line Discrimination) [13], which has been extended in [14],[15]. In general, passive remote sensing techniques can be partitioned into radiance-based (including FLD) and reflectance-based methods, e.g. using the physiological reflectance index (PRI) [16], where reflectance at  $531 nm$  and  $570 nm$  is used for indexing. For a more detailed description about passive remote sensing techniques the reader is referred to a more comprehensive review [17]. Lastly, there are long distance chlorophyll fluorescence sensing techniques, e.g. using satellite images to detect chlorophyll in cyanobacterial blooms [18] or globally identifying the functional status of vegetation [19].

## II. CHLOROPHYLL SENSOR DEVELOPMENT

We do not consider long distance sensing techniques as applicable for autonomous mowers. FLiDARs on the other hand can be used for accurately identifying the mowing area. However, since autonomous mowers are designed for low purchase and maintenance costs, FLiDARs in general are too expensive. Passive sensing might be a cost effective solution but requiring sunlight which limits its applicability, for example when the mowing time should be over night. The same argument holds for vision based systems which are in addition unreliable due to their statistical nature. To overcome these problems, i.e. low maintenance and acquisition costs, reliable detection of the mowing area and constant operational readiness, we propose our novel active chlorophyll sensor which

- (1) stimulates the chlorophyll fluorescence by emitting blue light with a standard 432 nm light emitting diode (LED).
- (2) detects the chlorophyll fluorescence response using a standard infrared phototransistor.
- (3) filtering the sunlight response by using high stimulation frequencies.

We start in Section II by summarizing the main aspects of chlorophyll fluorescence, Section II-A, from which we then derive the required design of our low-cost sensor, Section II-B. Furthermore, we then proceed to a theoretical consideration of the signal path, Section III. In Section IV, we shortly analyze the sensor components in order to define optimal operating settings. In the following, we evaluate the performance of the sensor statistically on grass collected samples, Section V-A, and with a mobile robot on an exemplary garden, Section V-B. We end with a discussion in Section VI and conclude in Section VII.

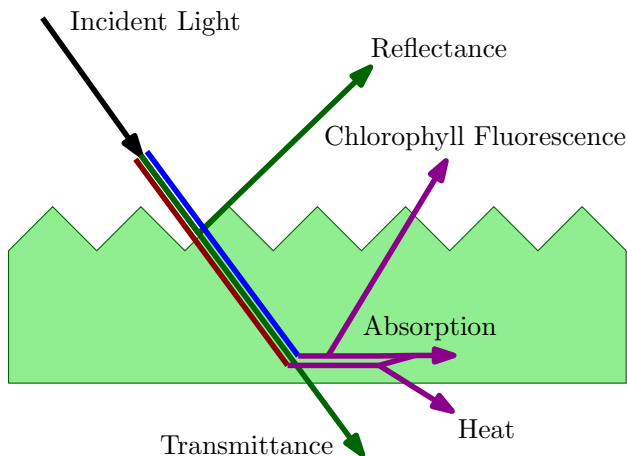


Fig. 2: Example diagram for Chlorophyll Fluorescence inspired by [20]. About 78% of the incident radiation is absorbed, while the rest is either transmitted or reflected. About 20% is dissipated through heat and only 2% emitted as fluorescence.

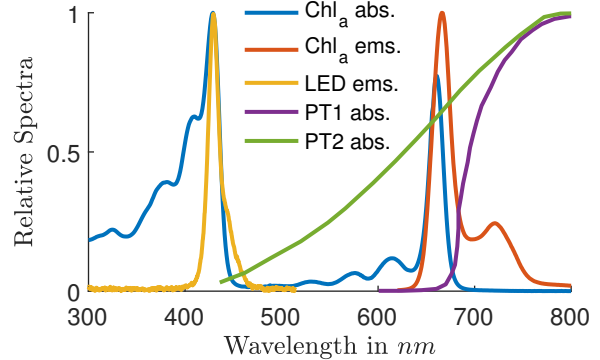


Fig. 3: Examples of different normalized absorption and emission spectra. The blue and red lines show the absorption and emission fluorescence spectra for Chlorophyll a in diethyl-ether taken from the PhotochemCAD database [23],[24]. The yellow line represents the measured emission spectrum of a consumer LED with emission peak at 432 nm. The purple and green lines show the spectral sensitivities for the RPT-37PB3F Phototransistor from Rohm Semiconductor and the PT480 from SHARP.

In this section, we investigate chlorophyll fluorescence as a unique feature of plants and grass. We first introduce the main concepts of chlorophyll fluorescence required for the sensor design, such as the absorption and emission fluorescence spectra, the “Kautsky-Effect” and the chlorophyll fluorescence life time. Based on the specific characteristics we then introduce a cost-efficient sensor design using available analog consumer electronic in combination with a small microcontroller.

### A. Chlorophyll Fluorescence Principle

We first review the main concepts in regard to chlorophyll fluorescence. For a detailed survey, we refer to [21] and [22]. Light energy absorbed by plants, more specifically by the chlorophyll molecules, can either drive photosynthesis reaction, it can be dissipated as heat or re-emitted as light which is called chlorophyll fluorescence, Figure 2. These three processes are in competition to each other, thus a decrease in efficiency at one process will increase the efficiency at another. In general, the light re-emitted by the chlorophyll fluorescence is of a magnitude much lower than the absorbed light, between 1 – 2%. However, since it is possible to stimulate chlorophyll fluorescence given a certain wavelength, it can be exploited for a sensor system. Therefore, the excitation wavelength has to be around 430 nm to optimally exploit the chlorophyll absorption spectrum, Figure 3, blue curve. The light re-emitted by the chlorophyll fluorescence is of longer wavelength with a peak at around 684 nm, Figure 3, red curve.

An important characteristic for chlorophyll fluorescence is the so called “Kautsky-Effect” [27], where a plant’s reaction to sudden light changes is investigated, e.g. the plant is unveiled in the sunlight. This change of setting results in an

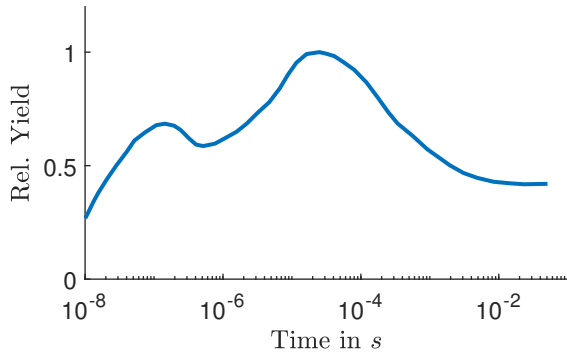


Fig. 4: The figure shows the chlorophyll a fluorescence yield change in the dark-adapted cells of the green alga *Chlorella* after a saturating nanosecond laser flash (adjusted from [25],[26]).

increase in the yield of chlorophyll fluorescence. This holds for the first second after which the fluorescence level drops down over a few minutes until it reaches a steady state. This drop down effect is known as fluorescence quenching [28]. In Figure 4, the “Kautsky-Effect” is shown which is induced by the photosystem II (PSII) [29] reaction centers being in a “closed” state. This decreases the photosynthesis process which on the other hand increases the chlorophyll fluorescence. Based on the “Kautsky-Effect”, certain effects such as plant stress can be measured by recording the relative fluorescence yield from plants even under full sunlight [30].

A much more important characteristic for our sensor design is the life time of chlorophyll fluorescence, which gives a lower bound for the sampling period of our sensor. The life time is thereby the time after stimulation in which chlorophyll fluorescence can be measured and lies around one nanosecond. For example, Schmuck and Moya [31] showed for spinach leaves that at steady state conditions the mean lifetime is  $0.415\text{ ns}$  and when closing all reaction centers of the PSII, thus enhancing chlorophyll fluorescence, the mean lifetime is around  $2\text{ ns}$ , see also Figure 5. Similar results have been achieved in [32] with maple and spinach leaves and in [33] with maize and spruce leaves.

### B. Core Sensor Design

As shown in Figure 3 the absorption spectrum of chlorophyll is particularly strong in the range around  $430\text{ nm}$ , whereas the emission spectrum is located in the area of  $650 - 750\text{ nm}$ . Thus, we require as stimulation source a consumer LED with emission peak at around  $430\text{ nm}$  and as absorption sink a standard phototransistor with a sufficient good spectral sensitivity between  $650 - 750\text{ nm}$ . Moreover, the emission spectrum of the chosen LED and the spectral sensitivity of the phototransistor should not overlap. Otherwise we can not distinguish between fluorescence response and LED radiation. The emission spectrum for the chosen LED (yellow) together with the spectral sensitivities for two different phototransistors

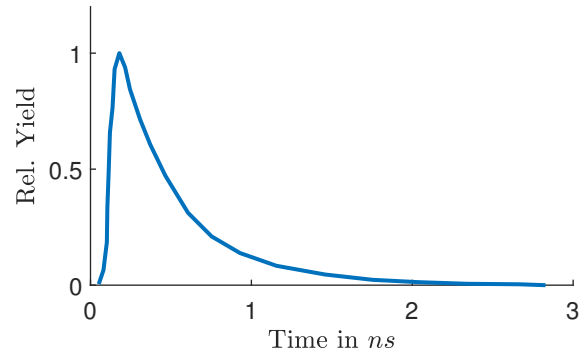


Fig. 5: The figure shows the chlorophyll fluorescence decay for a spinach leaf measured at  $684\text{ nm}$  after an excitation impulse with a width of  $70 - 80\text{ ps}$  (adjusted from [31]).

(purple, green) are drawn in Figure 3. The RPT-37PB3F has just a low spectral sensitivity in the desired area whereas the PT480 shows there high yield but intersects with the emission spectrum of the LED. Here, we use the RPT-37PB3F [34] since its spectral sensitivity does not intersect with the LED emission spectrum. In Figure 7, a detailed view of the spectral sensitivity and the resulting collector current with respect to the received illuminance is given.

In order to distinguish between the excited chlorophyll fluorescence and the ambient light (e.g. sunlight), the LED signal is modulated with a certain frequency  $f_{LED}$ . The current signal captured by the phototransistor is transformed using a current-to-voltage converter (transimpedance amplifier), the output voltage is further amplified and the resulting signal band pass filtered such that it is freed of ambient light influences.

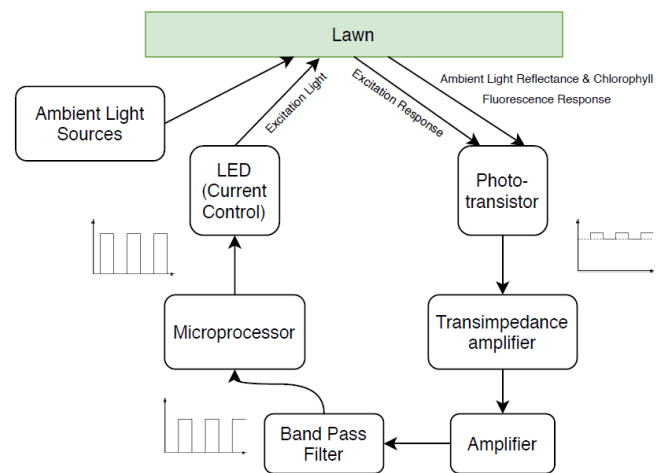
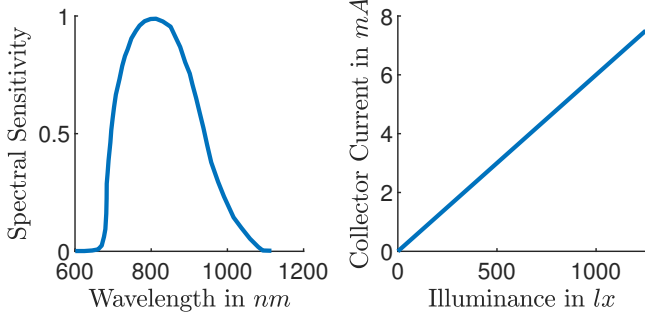


Fig. 6: The signal path for the proposed low cost sensor. The microprocessor controls the LED which emits a pulsed light for stimulating the chlorophyll process. The light radiated back is then absorbed by the PT and the result further processed and send back to the microprocessor for evaluation.



(a) Spectral sensitivity of the RPT-37PB3F with respect to the wavelength of the received light. (b) Resulting collector current with respect to the illuminance filtered by the spectral sensitivity.

Fig. 7: Spectral sensitivity and collector current of the RPT-37PB3F.

The control unit of the sensor is a small microprocessor, the *ATMEGA32U4* [35], which generates the excitation signal for the LED and receives the amplified and filtered chlorophyll fluorescence signal. To achieve high excitation frequencies, the in- and output signals are generated and captured by directly using interrupt routines. In addition, plastic lenses were used for emitting and receiving optics to focus the light onto and from the measurement area. The whole setting allows for high-volume lowest cost sensor.

### III. SIGNAL PATH ANALYSIS

We now analyze the signal path as presented in Figure 6, where we use the shorthand notation PT as acronym for phototransistor. We show that various parameters have to be considered when designing the sensor in order to achieve robust classification results, e.g. sensor apertures or electronic component characteristics. Parameters which play essential roles in the analysis are listed in Table I. While analyzing the signal path, we require different spectral functions  $f(\lambda)$  similar to those as shown in Figure 3, where  $\lambda$  is the wavelength. If we refer to function  $f(\lambda)$  as to be normalized, then

$$\int f(\lambda) d\lambda = 1, \quad (1)$$

and if we refer to function  $f(\lambda)$  as to be relative, then

$$f(\lambda) \in [0, 1] \quad \forall \lambda. \quad (2)$$

#### A. Sensor Apertures & Chlorophyll Fluorescence

In Figure 8, a sketch of the apertures for the LED and PT of the designed sensor are shown. Let  $\Phi_{LED}$  be the luminous flux of the LED. First, the light of the LED is conically sent to the grass and illuminates a certain area

$$A_{LED} = \pi (\tan(\beta_{LED}) h_{LED})^2, \quad (3)$$

where  $\beta_{LED}$  is the lens angle and  $h_{LED}$  the distance of the sensor to the ground. In order to estimate the resulting

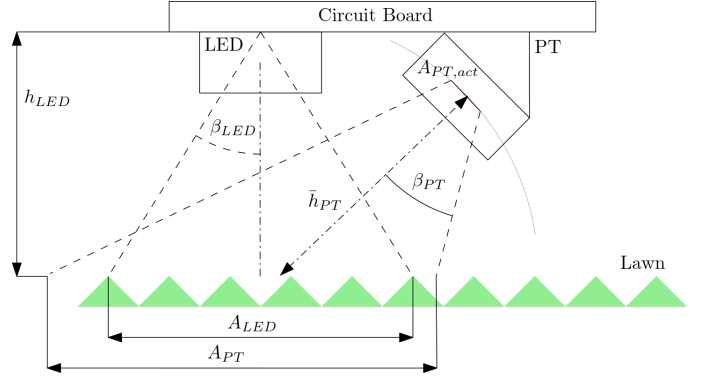


Fig. 8: A sketch of the sensor emission (LED) and absorption (PT) apertures. Optimally, the apertures are aligned to the same focus point with  $A_{LED} = A_{PT}$ .

luminous flux response of the chlorophyll to the PT we use the normalized emission spectrum,  $f_{LED}(\lambda)$ , and relative absorption spectrum,  $g_{Chl}(\lambda)$ , of the LED and chlorophyll *a* respectively in combination with the re-emission magnitude for chlorophyll fluorescence  $\gamma$ , which leads to

$$\Phi_{Chl} = \gamma \Phi_{LED} \int f_{LED}(\lambda) g_{Chl}(\lambda) d\lambda. \quad (4)$$

The amount of luminous flux from the chlorophyll fluorescence response received by the PT varies depending on the lens aperture. Here, we assume that PT's lens aperture is such positioned, that the complete illuminated area  $A_{LED}$  can be seen, which leads to a luminous flux from the chlorophyll fluorescence response into the the PT of

$$\Phi_{PT,AC} = \varphi \Phi_{Chl} \int f_{Chl}(\lambda) g_{PT}(\lambda) d\lambda. \quad (5)$$

Here,  $f_{Chl}(\lambda)$  is the normalized emission spectrum for the chlorophyll fluorescence,  $g_{PT}(\lambda)$  the relative spectral sensitivity of the PT and  $\varphi$  is the part of the scattered light from the lawn surface which is received by the PT. For calculating  $\varphi$ , we assume that the reflected scattered light is equally distributed in a half sphere from each point of the illuminated area. The distance between the active measurement surface  $A_{PT,act}$  and the illuminated area is  $h_{PT}$ , where  $h_{PT}$  differs with respect to the considered points of the active measurement surface and the illuminated area. To simplify our calculations, we assume that we can define a mean distance between the PT and the illuminated lawn area  $\bar{h}_{PT}$ . We then define  $\varphi$  as the part of the hemisphere of the emitted fluorescence which is received by the active measurement surface

$$\varphi = A_{PT,act} / (2\pi \bar{h}_{PT}^2). \quad (6)$$

#### B. Sun Radiation

In addition to the desired high frequency signal from the LED excitation, the PT also registers a low frequency signal from an ambient light source, the sun, which directly emits with  $E_{Sun}$ . To determine the amount of luminous flux reflected by grass and received by the PT, we use the surface Albedo

TABLE I: Important parameters for the analysis of the signal path.

Symbol	Value	Unit	Description
$A_{LED}$	$2.30 \times 10^{-3}$	$m^2$	illuminated area by the LED
$A_{PT}$	$3.40 \times 10^{-3}$	$m^2$	scanned area by the PT
$A_{PT,act}$	$7.55 \times 10^{-6}$	$m^2$	active measurement surface of the PT
$E_{Sun}$	$0 - 10^5$	$lx$	illuminance of the sun with $10^5$ by summer and clear sky
$f_{LED}$	38000	$Hz$	pulsing frequency of the LED
$f_{sensor}$	179	$Hz$	classification frequency of the sensor
$h_{LED}$	0.1	$m$	distance from the sensor to the ground
$h_{PT}$	0.12	$m$	mean distance between the PT and the illuminated area
$I_{C,AC}$	$2.7 \times 10^{-5}$	$A$	collector current of the PT, AC signal
$I_{C,DC}$	$0 - 3 \times 10^{-3}$	$A$	collector current of the PT, DC signal
$f_{LED}(\lambda)$	see Figure 3	1	normalized emission spectrum of the LED
$f_{Chl}(\lambda)$	see Figure 3	1	normalized emission spectrum of the chlorophyll fluorescence
$f_{Grass}(\lambda)$	see [36]	1	normalized reflection spectrum of grass
$g_{Chl}(\lambda)$	see Figure 3	1	relative absorption spectrum of chlorophyll a
$g_{PT}(\lambda)$	see Figure 3	1	relative spectral sensitivity of the PT
$\alpha$	0.25	1	surface Albedo
$\beta_{LED}$	15	$^\circ$	lens angle of the LED
$\gamma$	0.02	1	re-emission magnitude for the chlorophyll fluorescence
$\varphi$	$8.34 \times 10^{-5}$	1	part of scattered light from the lawn surface received by the PT
$\Phi_{LED}$	145	$lm$	luminous flux of the LED under full power
$\Phi_{Chl}$	2.112	$lm$	luminous flux from chlorophyll fluorescence response of the grass
$\Phi_{PT,AC}$	$3.39 \times 10^{-5}$	$lm$	luminous flux received by the PT, modulated AC signal
$\Phi_{PT,DC}$	$0 - 3.8 \times 10^{-3}$	$lm$	luminous flux received by the PT, sunlight DC signal

$\alpha \approx 0.25$  [37] and the normalized reflectance spectrum of grass  $f_{Grass}(\lambda)$  [36]. With the same assumptions and simplifications as above, we get

$$\Phi_{PT,DC} = \alpha \varphi E_{Sun} A_{PT} \int f_{Grass}(\lambda) g_{PT}(\lambda) d\lambda \quad (7)$$

for the luminous flux to the PT based on emitted sun radiation.

### C. Light Emission Acquisition

The luminous flux  $\Phi_{PT} = \Phi_{PT,DC} + \Phi_{PT,AC}$  induces a response of the PT, resulting in a collector current  $I_C$  based on the collector emitter voltage  $V_{CE}$  applied to the PT. For example, let  $V_{CE} = 5V$  then

$$I_C \approx \frac{3mA}{500lx} \frac{\Phi_{PT}}{A_{PT,act}}, \quad (8)$$

where the active measurement surface of the PT is given with  $A_{PT,act} = 7.55 mm^2$ . The AC part of the PT response generated by the pulsing LED is around  $I_{C,AC} \approx 27 \mu A$  whereas the the DC part increases linearly with increasing sun radiation, e.g. for  $E_{Sun} = 10^5 lx$  we get  $I_{C,DC} \approx 3mA$ . However, the *VSOP98260* [38] can only resolve currents up to  $400 \mu A$ . Thus, the maximum sun radiation with which the sensor works is around  $E_{Sun} = 10^4 lx$ . To solve this problem, the sensor can be shaded or a resistance bridge can be included to discharge part of the current. We discuss these options in more detail in Section VI. Finally, the *VSOP98260* amplifies and filters the signal and forwards it to the microprocessor.

### D. Signal Generation & Classification

Autonomous lawn mower in general move with a maximum velocity of  $v_{max} = 1 m/s$ . Given an area detection radius for the sensor of  $r_{LED} \approx 0.025 m$  and requiring an overlapping

between measurement areas of  $r_{LED}$ , the sensor's measurement frequency has to be at least

$$f_{sensor,min} = \frac{v_{max}}{r_{LED}} = 40 Hz. \quad (9)$$

Given the Bode plot and cut off frequency of the used LED, Figure 9b, a preamplifier circuit (*VSOP98260*) with a carrier frequency of  $f_{VSOP} = 38 KHz$  and a range for the pass band of  $20 KHz - 60 KHz$  is chosen. Thus, pulsing the LED with the carrier frequency  $f_{VSOP}$  exploits optimal the trade-off between high sampling frequencies and sensor light intensity. The chlorophyll fluorescence response speed lies around  $2 ns$ , Section II-A, and thus is with approximately  $500 MHz$  multiple orders of magnitude faster than our sensor. However, in order to ensure stability in the presence of measurement noise which might result to false positives or false negatives, we perform  $N = 200$  measurements. The sensor frequency then becomes

$$f_{sensor} = \frac{1}{N} f_{LED} - \epsilon \approx 180 Hz - \epsilon, \quad (10)$$

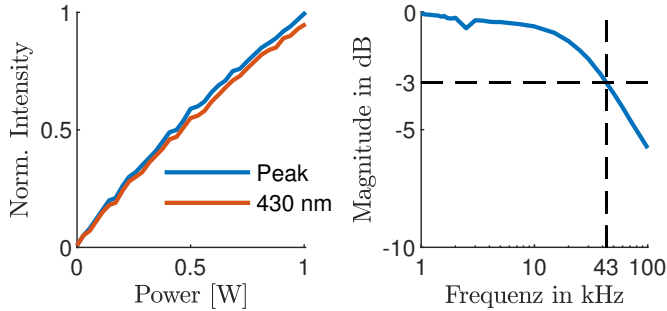
where  $\epsilon$  reflects the time required for sending the data over the serial connection during which no measurements are processed. Here, we got  $f_{sensor} \approx 179 Hz$  and thus  $\epsilon \approx 1 Hz$ . As classification result we get

$$c = \frac{n}{N}, \quad (11)$$

where  $n$  is the number of measured chlorophyll fluorescence responses within  $N$  LED pulses.

## IV. HARDWARE COMPONENT EVALUATION

We evaluated the individual components of the sensor in order to determine optimal settings in regard to range, ambient light tolerance and noise suppression.



(a) Relative light emission of the used high-power LED in proportion to the power consumption. (b) Bode plot for the LED in use. The cutoff frequency is at  $f_c = 43 \text{ kHz}$ .

Fig. 9: Relative light emission and Bode plot for the used high-power LED.

### A. Light Emission

For the light emission we use a high-power LED with 1 W maximum power consumption and a resulting luminous flux of approximately 145 lm. First, the LED was examined for its behavior with increasing power supply under constant current flow using the CCS200 spectrometer from *Thorlabs, Inc.* In Figure 9a, the measured data are depicted where the red curve shows the relative intensity at 430 nm and the blue curve the relative intensity at the peak of the measured spectrum. The emitted light intensity increases nearly linear with a small decrease in the slope. Second, we evaluated the frequency response of the LED measuring the light emission with a *BPX 65* photodiode connected to an oscilloscope (DSO6014A from *Agilent Technologies*). The photodiode has a rise and fall time of  $t_r, t_f = 0.012 \mu\text{s}$ . Thus, it can resolve a maximum frequency of 41,6 MHz. To drive the LED with different frequencies we used a programmable function generator (HM8131.2 from *HAMEG*). In Figure 9b, a bode plot for the LED emission is shown. The cutoff frequency here is approx.  $f_c = 43 \text{ kHz}$ .

### B. Fluorescence Detection

For the chlorophyll fluorescence signal detection we use infrared, high-sensitivity phototransistor, the RPT-37PB3F. First, we evaluated the frequency response of the PT with an oscilloscope (DSO6014A from *Agilent Technologies*) using a *OVP214VC* laser driven by the programmable function generator (HM8131.2 from *HAMEG*). The PT can easily reach the in the data sheet specified response (rise and fall) times of  $t_r = t_f = 10 \mu\text{s}$ . Hence, the PT is able to detect signals with a frequency up to  $f = 50 \text{ kHz}$  without loss of sensitivity. Second, we evaluated the saturation illuminance of the sensor, which is mainly limited by the maximum input current to the *VSOP98260*, Section III-C. The maximum utilization was achieved under direct light on the sensor at 3000 lx, which at an surface Albedo of 0.25 corresponds to a solar radiation of about 12000 lx. This is consistent with the previous calculations in Section III.

## V. SENSOR EVALUATION

The sensor was tested in 9 different garden environments, which have been sorted according to their visual grass quality, and on 3 different non-grass environments, see Figure 11. In total 280579 samples have been collected. In addition, the sensor was tested on a mobile robot where an exemplary garden was scanned.

### A. Statistical Analysis in 9 different Garden Environments

We collected samples in 9 different lawn environments by attaching the sensor onto a lawn mower. For each lawn type approximately 23500 samples have been collected. In addition, data samples for 3 non-grass environments have been collected in order to analyze sensor noise. The non-grass as well as the grass environments are shown in Figure 11, where we classified them according to their visual grass quality. Here, a grass quality of 1 represents the lowest grass quality and 9 the highest. The sensor noise, analyzed by evaluating the sensor results collected on the non-lawn environments, approximated as a normal distribution has a mean classification result of  $\mu \approx 0.177$  and a standard deviation of  $\sigma \approx 0.051$ . Defining a positive classification result (grass detection) as  $c > \mu + 3\sigma$ , results in exclusion of nearly all false positive results, since 99.73% of all errors are within the  $\mu \pm 3\sigma$  region. In Figure 10a, a histogram for the classification values  $c$  for the non-grass measurements are shown.

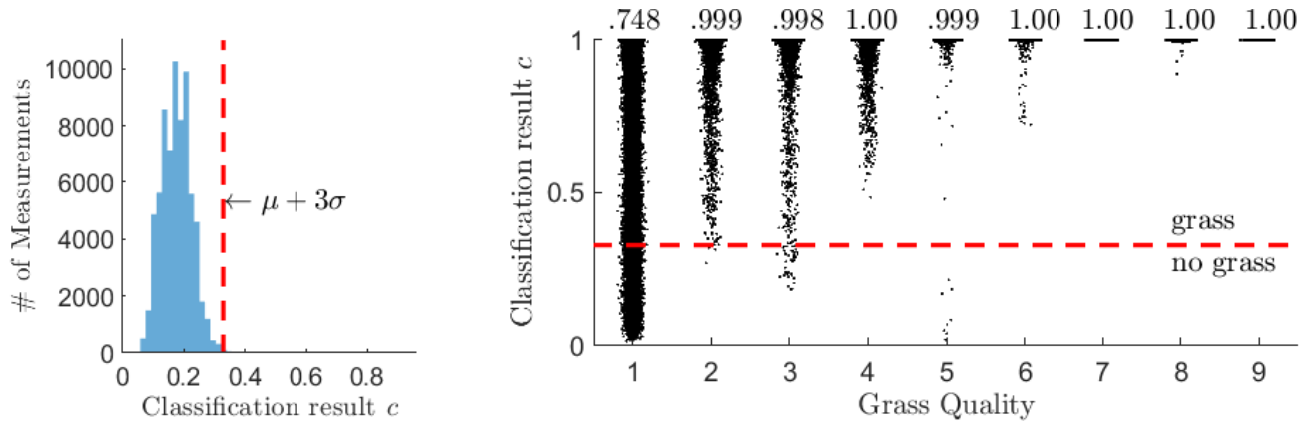
Based on the  $\mu + 3\sigma$  decision boundary, we can now decide when grass has been detected. In Figure 10b, the classification results  $c$  for the different lawn environments are shown, where we inflated the grass-quality values with some random noise for better readability. Above each lawn type, we added the classification accuracy, thus the amount of correctly classified samples, which already have been shown in Figure 1a. All of the different lawn types reach approximately 100% accurate classification results except the lawn with the lowest quality, which still reach a classification accuracy of approximately 75%.

### B. Mowing Area Classification

We tested the proposed chlorophyll fluorescence sensor in a realistic garden environment on an autonomous lawn mower. For the localization of the lawn mower we used the real-time locating system (RTLS) MDEK1001 from *Decawave*. In Figure 12, the relative classification results  $c$  are shown. Figure 12a shows the evaluated section of the garden environment from the bird's eye perspective and Figure 12b the interpolated sensor measurements. The proposed chlorophyll fluorescence sensor reliably detects grass and thus the working space for the autonomous lawn mower.

## VI. DISCUSSION

As demonstrated in Section V, our chlorophyll fluorescence sensor is able to reliably detect grass and thus classify the



(a) The classification results  $c$  for the non-lawn environments with a mean and standard deviation of  $\mu = 0.177$  and  $\sigma = 0.051$ . The  $\mu + 3\sigma$  decision line for grass detection is shown in red. (b) The classification results  $c$  for the 9 different lawn environments, where the environments are sorted based on their visual grass quality with 1 being the lowest and 9 the highest grass quality. Above each lawn category the amount of correctly classified measurements is shown.

Fig. 10: Statistical evaluation of the chlorophyll fluorescence sensor on 9 different lawn and 3 different non-lawn environments, Figure 11, given the classification results  $c$  defined in Equation (11). The sensor shows stable and reliable classification results with approximately 100 % accuracy for different lawn types, except for the lawn with the lowest quality, whereas even for such grass an accuracy of approximately 75 % could be reached.

working area for autonomous lawn mowers. However, there are three issues we like to discuss: the limitation due to high sun radiation mentioned in Section III-C, the measurement noise of the sensor shown in Figure 10a and further possible fields of application for the presented sensor.

#### A. Limitation due to High Sun Radiation

The limitation due to high sun radiation comes from the choice of sensor components and the design itself. Possible workarounds are to shade the grass sensor, add a resistor bridge to discharge a part of the current or choose other electronic components with larger resolvable currents. Shading the sensor might be not always possible, especially if the sensor is placed at the front of the lawn mower where bumper sensor are also often situated. Adding a resistor bridge to discharge a part of the current leads to better performance under high sun radiation but due to the current discharging, we get problems for low sun radiation, e.g. measuring at night. During the development of the sensor we tested various electronic components, such as different LEDs and PTs. Keeping in mind our low-cost approach, the proposed design fulfills our requirements to the best of our knowledge.

#### B. Sensor Measurement Noise

Following the physical principle of chlorophyll fluorescence, an ideal sensor should not detect anything if sensing non-grass environments. However, we saw that there is some measurement noise caused by several error sources, e.g. non-ideal emission and absorption spectra of the LED and the PT or noise of the individual electronic components due to voltage

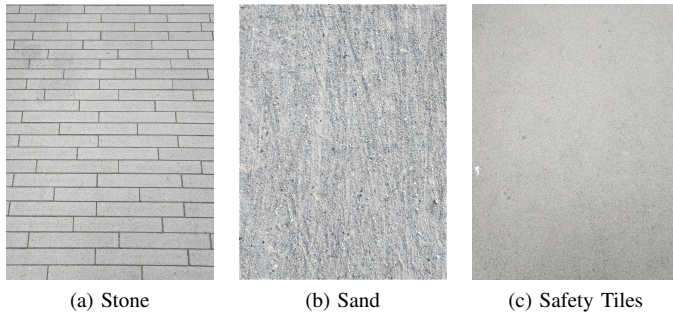
or current fluctuations. We reduced these errors to the best of our knowledge to ensure reliable detection of grass, keeping in mind our low-cost approach. For example, we continuously improved the design of the printed circuit board (PCB).

#### C. Fields of Application

As mentioned in the introduction, we designed the sensor as mowing area classifier for autonomous lawn mower. However, the proposed sensor is not restricted to this field of application. Rather, all areas in which chlorophyll fluorescence plays a role can be considered as possible fields of application, e.g. agriculture or gardening in general. For example, plant stress recognition, which is of high importance in modern agriculture, can be measured by exploiting the “Kautsky-Effect” as demonstrated in [30]. Such plant stress measuring systems have been introduced in [39] or [40]. However, current systems require an enclosure around the plant for executing the measurements. By adapting our sensor design, plant stress recognition can be potentially added as new feature.

## VII. CONCLUSION

We proposed a low-cost sensor approach using chlorophyll fluorescence for working space detection for autonomous lawn mowers. We demonstrated, that our sensor produces stable and reliable results for grass detection by collecting multiple samples on lawns with different grass quality. Furthermore, we showed that our sensor reliably detects the lawn area under real life conditions by evaluating the sensor in a realistic garden environment. Due to the low-cost approach, our proposed sensor allows to develop more cost-effective garden robots. In further steps, we will compare our sensor with the currently used perimeter sensors on autonomous lawn mowers.



(a) Stone

(b) Sand

(c) Safety Tiles



(d) Quality 1

(e) Quality 2

(f) Quality 3



(g) Quality 4

(h) Quality 5

(i) Quality 6



(j) Quality 7

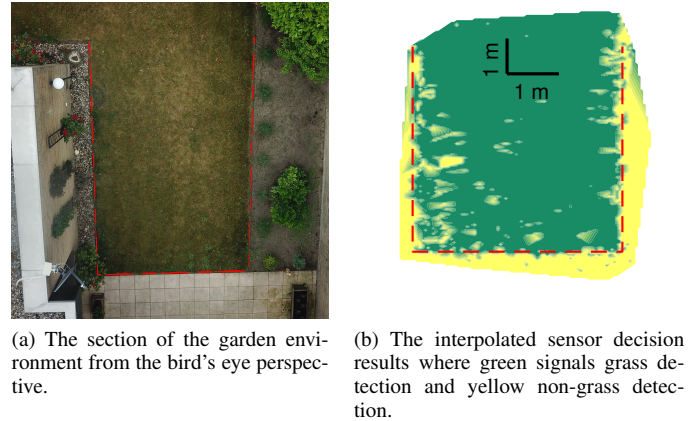
(k) Quality 8

(l) Quality 9

Fig. 11: Different lawn types, sorted and classified based on the observable relative quality.

## REFERENCES

- [1] J. Yang, S.-J. Chung, S. Hutchinson, D. Johnson, and M. Kise, "Vision-based localization and mapping for an autonomous mower," in *2013 IEEE/RSJ International Conference on Intelligent Robots and Systems*. IEEE, 2013, pp. 3655–3662.
- [2] T. Fukukawa, K. Sekiyama, Y. Hasegawa, and T. Fukuda, "Vision-based mowing boundary detection algorithm for an autonomous lawn mower," *Journal of Advanced Computational Intelligence and Intelligent Informatics*, vol. 20, no. 1, pp. 49–56, 2016.
- [3] F. Bernini, "Lawn-mower with sensor," Nov. 3 2009, uS Patent 7,613,552.
- [4] U. Watchareeruetai, Y. Takeuchi, T. Matsumoto, H. Kudo, and



(a) The section of the garden environment from the bird's eye perspective.

(b) The interpolated sensor decision results where green signals grass detection and yellow non-grass detection.

Fig. 12: Evaluation results for the chlorophyll fluorescence sensor under real garden conditions.

- N. Ohnishi, "Computer vision based methods for detecting weeds in lawns," *Machine Vision and Applications*, vol. 17, no. 5, pp. 287–296, 2006.
- [5] A. Schepelmann, R. E. Hudson, F. L. Merat, and R. D. Quinn, "Visual segmentation of lawn grass for a mobile robotic lawnmower," in *2010 IEEE/RSJ International Conference on Intelligent Robots and Systems*. IEEE, 2010, pp. 734–739.
- [6] A. D. Smith, H. J. Chang, and E. J. Blanchard, "An outdoor high-accuracy local positioning system for an autonomous robotic golf greens mower," in *2012 IEEE International Conference on Robotics and Automation*. IEEE, 2012, pp. 2633–2639.
- [7] S. L. Bellinger, "Self-propelled random motion lawnmower," Mar. 16 1971, uS Patent 3,570,227.
- [8] N. Rottmann, R. Bruder, A. Schweikard, and E. Rueckert, "Exploiting chlorophyll fluorescence for building robust low-cost mowing area detectors," in *IEEE SENSORS*, 2020, pp. 1–4. [Online]. Available: <https://ai-lab.science/wp/IEEESensors2020Rottmann.pdf>, ArticleFile
- [9] I. Moya and Z. G. Cerovic, "Remote sensing of chlorophyll fluorescence: instrumentation and analysis," in *Chlorophyll a Fluorescence*. Springer, 2004, pp. 429–445.
- [10] F. Castagnoli, G. Cecchi, L. Pantani, I. Pippi, B. Radicati, and P. Mazzinghi, "A fluorescence lidar for land and sea remote sensing," in *Laser Radar Technology and Applications I*, vol. 663. International Society for Optics and Photonics, 1986, pp. 212–216.
- [11] J. Yang, W. Gong, S. Shi, L. Du, B. Zhu, J. Sun, and S. Song, "Excitation wavelength analysis of laser-induced fluorescence lidar for identifying plant species," *IEEE Geoscience and Remote Sensing Letters*, vol. 13, no. 7, pp. 977–981, 2016.
- [12] G. Samson, N. Tremblay, A. Dudelzak, S. Babichenko, L. Dextraze, and J. Wollring, "Nutrient stress of corn plants: early detection and discrimination using a compact multiwavelength fluorescent lidar," in *Proceedings of the 20th EARSeL Symposium, Dresden, Germany*, 2000, pp. 214–223.
- [13] J. A. Plascyk, "The mk ii fraunhofer line discriminator (fld-ii) for airborne and orbital remote sensing of solar-stimulated luminescence," *Optical Engineering*, vol. 14, no. 4, p. 144339, 1975.
- [14] I. Moya, L. Camenen, G. Latouche, C. Mauxion, S. Evain, and Z. Cerovic, "An instrument for the measurement of sunlight excited plant fluorescence," in *Photosynthesis: mechanisms and effects*. Springer, 1998, pp. 4265–4270.
- [15] P. L. Kebabian, A. F. Theisen, S. Kallelis, and A. Freedman, "A passive two-band sensor of sunlight-excited plant fluorescence," *Review of Scientific Instruments*, vol. 70, no. 11, pp. 4386–4393, 1999.
- [16] J. Gamon, J. Penuelas, and C. Field, "A narrow-waveband spectral index that tracks diurnal changes in photosynthetic efficiency," *Remote Sensing of environment*, vol. 41, no. 1, pp. 35–44, 1992.
- [17] M. Meroni, M. Rossini, L. Guanter, L. Alonso, U. Rascher, R. Colombo, and J. Moreno, "Remote sensing of solar-induced chlorophyll fluorescence: Review of methods and applications," *Remote Sensing of Environment*, vol. 113, no. 10, pp. 2037–2051, 2009.

- [18] T. Kutser, "Quantitative detection of chlorophyll in cyanobacterial blooms by satellite remote sensing," *Limnology and Oceanography*, vol. 49, no. 6, pp. 2179–2189, 2004.
- [19] J. Joiner, Y. Yoshida, A. Vasilkov, E. Middleton, *et al.*, "First observations of global and seasonal terrestrial chlorophyll fluorescence from space," *Biogeosciences*, vol. 8, no. 3, pp. 637–651, 2011.
- [20] M. Davidson, M. Berger, I. Moya, J. Moreno, T. Laurila, M.-P. Stoll, and J. Miller, "Mapping photosynthesis from space—a new vegetation-fluorescence technique," *ESA bulletin*, vol. 116, pp. 34–37, 2003.
- [21] K. Maxwell and G. N. Johnson, "Chlorophyll fluorescence—a practical guide," *Journal of experimental botany*, vol. 51, no. 345, pp. 659–668, 2000.
- [22] H. M. Kalaji, G. Schansker, M. Brestic, F. Bussotti, A. Calatayud, L. Ferroni, V. Goltsev, L. Guidi, A. Jajoo, P. Li, *et al.*, "Frequently asked questions about chlorophyll fluorescence, the sequel," *Photosynthesis Research*, vol. 132, no. 1, pp. 13–66, 2017.
- [23] M. Taniguchi, H. Du, and J. S. Lindsey, "Photochemcad 3: diverse modules for photophysical calculations with multiple spectral databases," *Photochemistry and photobiology*, vol. 94, no. 2, pp. 277–289, 2018.
- [24] M. Taniguchi and J. S. Lindsey, "Database of absorption and fluorescence spectra of 300 common compounds for use in photochem cad," *Photochemistry and photobiology*, vol. 94, no. 2, pp. 290–327, 2018.
- [25] D. Mauzerall, "Light-induced fluorescence changes in chlorella, and the primary photoreactions for the production of oxygen," *Proceedings of the National Academy of Sciences*, vol. 69, no. 6, pp. 1358–1362, 1972.
- [26] G. Jee, "Sixty-three years since kautsky: chlorophylla fluorescence," *Aust. J. Plant Physiol.*, vol. 22, pp. 131–160, 1995.
- [27] H. Kautsky and A. Hirsch, "New attempts for carbon dioxide assimilation," *Naturwissenschaft*, vol. 19, pp. 964–964, 1931.
- [28] J. R. Lakowicz, "Quenching of fluorescence," in *Principles of fluorescence spectroscopy*. Springer, 1983, pp. 257–301.
- [29] A. Rutherford and P. Faller, "Photosystem ii: evolutionary perspectives," *Philosophical Transactions of the Royal Society of London. Series B: Biological Sciences*, vol. 358, no. 1429, pp. 245–253, 2003.
- [30] U. Schreiber and W. Bilger, "Rapid assessment of stress effects on plant leaves by chlorophyll fluorescence measurements," in *Plant response to stress*. Springer, 1987, pp. 27–53.
- [31] G. Schmuck and I. Moya, "Time-resolved chlorophyll fluorescence spectra of intact leaves," *Remote sensing of environment*, vol. 47, no. 1, pp. 72–76, 1994.
- [32] F. Pellegrino, A. Dagen, P. Sekuler, and R. Alfano, "Temperature dependence of the 735 nm fluorescence kinetics from spinach measured by picosecond laser-streak camera system," *Photobiochemistry and photobiophysics*, 1983.
- [33] M. Senoner, "The nanosecond decay of variable chlorophyll fluorescence in leaves of higher plants," *Biochimica et Biophysica Acta (BBA)-Bioenergetics*, vol. 849, no. 3, pp. 374–380, 1986.
- [34] *RPT-37PB3F Datasheet*, ROHM Semiconductor, 2018, rev. 2018.06. [Online]. Available: [https://fscdn.rohm.com/en/products/databook/datasheet/opto/optical\\_sensor/photo\\_transistor/rpt-37pb3f-e.pdf](https://fscdn.rohm.com/en/products/databook/datasheet/opto/optical_sensor/photo_transistor/rpt-37pb3f-e.pdf)
- [35] *ATmega16U4/ATmega32U4 Datasheet*, Atmel, april 2016. [Online]. Available: [http://ww1.microchip.com/downloads/en/DeviceDoc/Atmel-7766-8-bit-AVR-ATmega16U4-32U4\\_Datasheet.pdf](http://ww1.microchip.com/downloads/en/DeviceDoc/Atmel-7766-8-bit-AVR-ATmega16U4-32U4_Datasheet.pdf)
- [36] R. Clark, G. Swayze, R. Wise, K. Livo, T. Hoefen, R. Kokaly, and S. Sutley, "Usgs digital spectral library splib05a. usgs open-file report 03-395," *US Geological Survey: Reston, VA, USA*, 2003. [Online]. Available: <https://pubs.usgs.gov/of/2003/ofr-03-395/datatable.html>
- [37] J. Bray, J. Sanger, and A. Archer, "The visible albedo of surfaces in central minnesota," *Ecology*, vol. 47, no. 4, pp. 524–531, 1966.
- [38] *VSOP98260 Datasheet*, Vishay Semiconductor, march 2020, rev. 2.1. [Online]. Available: <https://www.vishay.com/docs/82447/vsop98260.pdf>
- [39] R. Lussier, "Bio-imaging and information system for scanning, detecting, diagnosing and optimizing plant health," Sept. 26 2006, uS Patent 7,112,806.
- [40] —, "Portable intelligent fluorescence and transmittance imaging spectroscopy system," Aug. 21 2012, uS Patent 8,249,308.



**Nils Rottmann** With January 2018, Nils Rottmann is a PhD student and research scientist at the Institute for Robotics and Cognitive Systems at the University of Luebeck. In his doctoral study, with the title "Learning Optimal Control and Planning Strategies in Mobile and Humanoid Robots", he develops low-cost sensor systems and investigates probabilistic learning and modeling approaches. He holds a master degree in Theoretical Mechanical Engineering from the Hamburg University of Technology, Germany.



**Ralf Bruder** Ralf Bruder studied Mathematics and Computer Science at the Westfälische Wilhelmsuniversität Münster and Technische Universität Clausthal. In 2006, he joined the Institute for Robotics and Cognitive Systems, where he develops medical sensor systems for automated interventions.



**Achim Schweikard** Achim Schweikard studied Mathematics at Hamburg University and University of Paris XI. He obtained his PhD from Technical University of Berlin in 1989. In 1994 he joined Technical University of Munich (TU Munich) as an Associate Professor. In 2002 he joined Luebeck University as a Full Professor. He is the inventor of numerous technologies in medical robotics.



**Elmar Rueckert** Elmar Rueckert is professor of Robotics at the University of Luebeck. He received his PhD in computer science at the Graz University of Technology in 2014 and worked for four years as senior researcher and research group leader at the Technical University of Darmstadt. His research interests includes stochastic machine and deep learning, robotics and reinforcement learning and medical and human motor control. In 2019, he won the 'German Young Researcher Award'.